

# 1 Advanced properties of CMOS current mirrors

## 1.1 Current Mirrors: Frequency response.

Current mirrors are often used to process signals in the form of variable currents. In these cases, it is important to know the frequency response between the input and the output currents. The typical configuration is shown in Fig.1.1. The input current is provided by an ideal current source, while the output current flows into the ideal voltage source  $V_{out}$ . In terms of small signal analysis, this means that we are considering the output short circuit current. In real cases, the output terminal of the mirror is connected to a non-zero load impedance, so that a current divider is formed by the output impedance of the mirror and the load impedance. Whenever the load impedance is much smaller than the mirror output impedance, we can consider that the whole output short circuit current actually flows into the load.

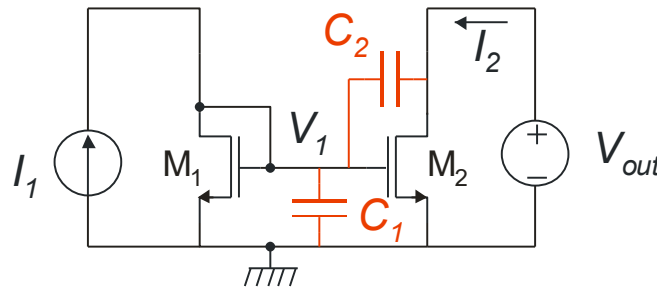


Fig.1.1. Simple MOSFET current mirror with parasitic capacitances.

In order to study the frequency response, the parasitic capacitors  $C_1$  and  $C_2$  shown in Fig. 1.1 should be taken into account. They are given by:

$$\begin{aligned} C_1 &= C_{GS1} + C_{GS2} + C_{DB1} \\ C_2 &= C_{GD2} \end{aligned} \tag{1.1}$$

The small signal model of the mirror is shown in Fig.1.2, where the diode-connected device  $M_1$  has been replaced by its equivalent resistance, given by the parallel of  $1/g_{m1}$  with  $r_{d1}$ , which is nearly equal to  $1/g_{m1}$

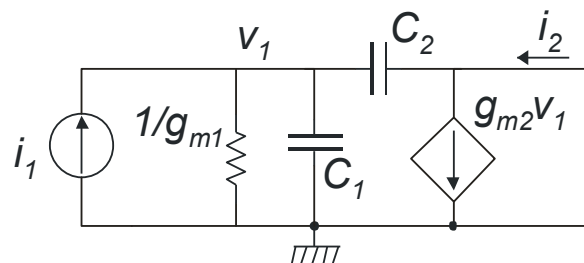


Fig. 1.2. Small signal equivalent circuit of a current mirror

The following expression for voltage  $v_1$  and current  $i_2$  can be easily found:

$$v_1 = i_1 \left( \frac{1}{g_{m1} + s(C_1 + C_2)} \right) \tag{1.2}$$

$$i_2 = v_1 g_{m2} - v_1 s C_2 \tag{1.3}$$

Substituting  $v_1$  into (1.3), we get the transfer function  $A_I = i_2/i_1$  (small-signal current-gain of the mirror):

$$A_I = \left( \frac{g_{m2} - sC_2}{g_{m1} + s(C_1 + C_2)} \right) = \frac{g_{m2}}{g_{m1}} \left( \frac{1 - \frac{s}{\omega_z}}{1 + \frac{s}{\omega_p}} \right) = A_I(0) \left( \frac{1 - \frac{s}{\omega_z}}{1 + \frac{s}{\omega_p}} \right) \tag{1.4}$$

The pole ( $\omega_p$ ) and zero ( $\omega_z$ ) angular frequencies are given by:

$$\omega_p = \frac{g_{m1}}{C_1 + C_2} \cong \frac{g_{m1}}{C_1} \qquad \omega_z = \frac{g_{m2}}{C_2} \tag{1.5}$$

The approximation of  $\omega_p$  is due to the fact that, considering (1.1), typically:  $C_2 \ll C_1$ . The ratio  $g_{m2}/g_{m1}$  is the DC gain of the mirror, indicated with  $A_I(0)$ , which, in the ideal case, is equal to the nominal gain  $k_M$  of the mirror, where  $k_M = W_2 L_1 / W_1 L_2$ . Clearly, due to systematic (e.g. effect of  $r_{d1}$ ) and random non idealities, the actual DC gain  $A_I(0)$  and the nominal gain may be slightly different.

The frequency response of the current gain is then represented by the asymptotic curves shown in Fig.1.3 (bode plots), where it has been assumed that  $A_I(0)$ , is greater than one. Note that the zero is positive, so that it gives a negative phase contribution, like the pole. The total asymptotic phase delay of a current mirror is then  $180^\circ$ . When the frequency tends to infinity,  $v_1$  tends to zero, and so does the current  $g_{m2}v_1$ . Therefore, the high frequency limit of the gain,  $A_I(\infty)$ , is due only to the capacitive current divider formed by  $C_1$  and  $C_2$ , so that

$$|A_I(\infty)| = \frac{C_2}{C_1 + C_2} \ll 1 \tag{1.6}$$

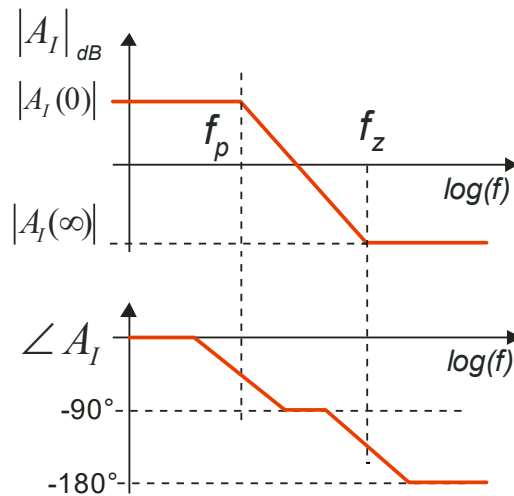


Fig. 1.3 Typical asymptotic magnitude and phase response of a current mirror.

As a result, if the DC gain of the mirror is greater than one or even slightly lower than one, the frequency of the pole is lower than that of the zero. Mirrors with a unity current gain represent the most frequent case of current mirror applications: they are characterized by a frequency response similar to that of Fig.1.3, with only the exception that  $A_I(0)$  is 0 dB. Only in the case of mirrors designed to have a gain much smaller than one the pole and zero may be swapped along the frequency axis, as shown in Fig.1.4.

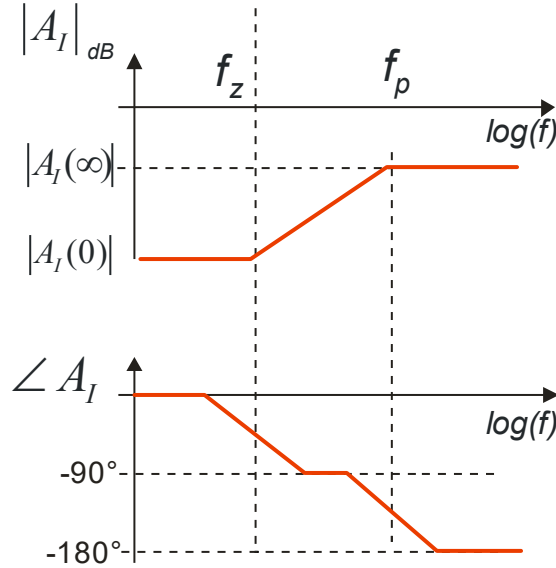


Fig.1.4. Frequency response of current mirror in the case that the nominal current gain is  $\ll 1$

As mentioned above, in most cases the singularity with lower characteristic frequency is the pole, so that the upper frequency limit of the mirror is given by the pole frequency  $f_p$ .

Considering Eq. (1.5) and using the strong inversion approximation for  $g_{m1}$ :

$$f_p = \frac{\omega_p}{2\pi} \cong \frac{1}{2\pi} \frac{g_{m1}}{C_1} = \frac{1}{2\pi} \frac{\mu C_{ox}}{C_1} \frac{W}{L} (V_{GS} - V_t) \quad (1.7)$$

Neglecting  $C_{DB}$  with respect to  $C_{GS1} + C_{GS2}$  in the expression of  $C_1$ , we get the expression:

$$f_p \cong \frac{1}{2\pi} \frac{\mu C_{ox} \frac{W_1}{L_1} (V_{GS} - V_t)}{\frac{2}{3} C_{ox} (W_1 L_1 + W_2 L_2)} = \frac{\frac{3}{4\pi} \mu \frac{1}{L_1} (V_{GS} - V_t)}{\left(1 + \frac{W_2 L_2}{W_1 L_1}\right)} = \frac{f_{T1}}{\left(1 + \frac{W_2 L_2}{W_1 L_1}\right)} \quad (1.8)$$

Where  $f_{T1}$  is the transition frequency of  $M_1$ , i.e. the frequency at which the current gain of  $M_1$  becomes one. Note that the actual pole frequency is slightly lower than the value given by (1.8), due to the fact that we have neglected the drain-body capacitance of  $M_1$  and capacitance  $C_2$ , equal to  $C_{db2}$ .

In the case of a mirror with nominal unity current gain,  $M_1$  and  $M_2$  are identical, so that the upper band limit is half the transition frequency. For mirrors with current gains different from one, we need to know how  $M_1$  and  $M_2$  are designed. An important case is that of precision mirrors, where  $M_1$  and  $M_2$  have the same length. In this case, indicating with  $k_M$  the nominal current gain of the mirror, we have:

$$L_1 = L_2 \Rightarrow \begin{cases} k_M = \frac{W_2}{L_2} \frac{L_1}{W_1} = \frac{W_2}{W_1} \\ \frac{W_2 L_2}{W_1 L_1} = \frac{W_2}{W_1} = k_M \end{cases} \quad (1.9)$$

Therefore, for precision mirrors, (1.8) becomes:

$$f_p \cong \frac{f_{T1}}{(1+k_M)} \quad (1.10)$$

To summarize:

- The frequency response of a current mirror is marked by a pole and a positive zero. The total asymptotic phase delay introduced by the pole-zero pair is  $180^\circ$ . This aspect should be carefully taken into account when current mirrors are present in the signal path. Critical stability issues may occur in feedback loops that include current mirrors.
- In most current mirrors, including the frequent case of mirrors with unity nominal gain, the pole frequency is lower than the zero one, so that the upper frequency limit is given by  $f_p$ , which is of the same order of magnitude as the transition frequency of  $M_1$ .
- The transition frequency shows an inverse proportionality to  $L_1^2$ , so that mirrors formed by long MOSFETs have a poor frequency response. In order to improve the frequency response,  $V_{GS}-V_T$  should be made large, with obvious drawbacks in terms of minimum output voltage ( $V_{min}$ ).
- If  $M_1$  and  $M_2$  have the same length, as typically occurs when precise current gains ( $k_M$ ) are required, the pole frequency is given by  $f_T$  divided by  $1+k_M$ . Therefore: the higher the current gain, the lower the mirror bandwidth.
- Mirrors with a particularly low nominal DC gain may be marked by a zero frequency lower than the pole one ( $f_z < f_p$ ). Since, in terms of phase delay, the zero behaves like the pole, the upper band limit will be given by the zero. This fact should be taken into account when designing feedback loops that include mirrors with a gain much lower than one.

### 1.2 Current Mirrors: noise.

The output current noise of a current mirror can be calculated with the small signal circuit of Fig. 1.5, where the noise currents  $i_{n1}$  and  $i_{n2}$  of  $M_1$  and  $M_2$ , respectively, have been highlighted. Comparison with the circuit of Fig.1.1 shows that the input source  $I_1$  has been removed, since here we are concerned with the effects of noise sources. The voltage source  $V_{out}$  has also been replaced with a short circuit to ground, since we are dealing only with small signals. Parasitic capacitances have been neglected since only noise components at frequencies much lower than the upper frequency limit are considered.

The output current is given by:

$$i_2 = i_{n2} - A_I(0)i_{n1} \tag{1.11}$$

The power spectral density (PSD) of the output current  $i_2$ , indicated with  $S_{Iout}$ , is given by:

$$S_{Iout}(f) = S_{In2}(f) + |A_I(0)|^2 S_{In1}(f) \cong S_{In2}(f) + \left(\frac{g_{m2}}{g_{m1}}\right)^2 S_{In1}(f) \tag{1.12}$$

where  $S_{In1}$  and  $S_{In2}$  are the PSDs of  $i_{n1}$  and  $i_{n2}$ , respectively.

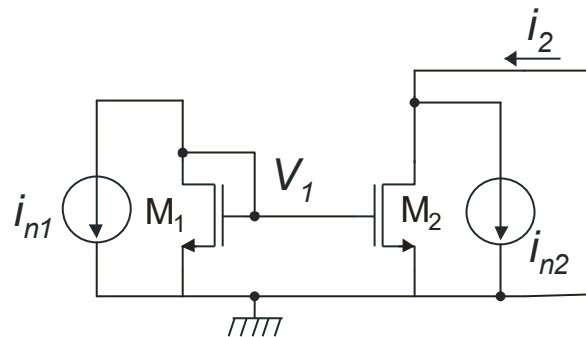


Fig.1.5. Current mirror with noise sources of the input and output device

In the case of thermal noise, the following expression for the MOSFET current noise PSD will be assumed:

$$S_{in}(f) = \frac{8}{3} kTg_m \quad (\text{thermal noise component}) \tag{1.13}$$

where  $k$  is the Boltzmann constant and  $T$  the absolute temperature. Substituting (1.13) into (1.12) for both currents  $i_1$  and  $i_2$ , the total thermal noise PSD of the output current ( $S_{ITh}$ ) becomes:

$$S_{Ith}(f) = \frac{8}{3} kTg_{m2} + \left(\frac{g_{m2}}{g_{m1}}\right)^2 \frac{8}{3} kTg_{m1} = \frac{8}{3} kTg_{m2} \left(1 + \frac{g_{m2}}{g_{m1}}\right) \quad (1.14)$$

Considering that  $g_{m2}/g_{m1} \cong A_I(0) \cong k_M$ , Eq. (1.14) becomes:

$$S_{Ith}(f) = \frac{8}{3} kTg_{m2}(1 + k_M) \quad (1.15)$$

Substituting:  $g_{m2} = I_{D2}/V_{TE2} = I_{out}/V_{TE2}$  we get:

$$S_{Ith}(f) = \frac{8}{3} kT \frac{I_{out}}{V_{TE2}} (1 + k_M) \quad (1.16)$$

In the case of flicker noise, the following expression of the MOSFET current noise PSD can be adopted:

$$S_{in}(f) = g_m^2 \frac{N_f}{WL} \frac{1}{f} \quad (\text{flicker noise component}) \quad (1.17)$$

where  $N_f$  is the flicker noise constant (process parameter). The flicker component ( $S_{IF}$ ) of the output noise PSD is given by:

$$\begin{aligned} S_{IF}(f) &= g_{m2}^2 \frac{N_f}{W_2 L_2} \frac{1}{f} + \left(\frac{g_{m2}}{g_{m1}}\right)^2 g_{m1}^2 \frac{N_f}{W_1 L_1} \frac{1}{f} = \\ &= \frac{g_{m2}^2 N_f}{f} \left(\frac{1}{W_2 L_2} + \frac{1}{W_1 L_1}\right) = g_{m2}^2 \frac{N_f}{W_2 L_2} \left(1 + \frac{W_2 L_2}{W_1 L_1}\right) \frac{1}{f} \end{aligned} \quad (1.18)$$

In the case that  $L_1 = L_2$ , considering relationships (1.9), Eq.(1.18) can be rewritten:

$$S_{IF}(f) = g_{m2}^2 \frac{N_f}{W_2 L_2} (1 + k_M) \frac{1}{f} \quad (1.19)$$

Similarly to the case of thermal noise, we write  $g_{m2}$  as a function of  $I_{out}$  and  $V_{TE2}$ , obtaining:

$$S_{IF}(f) = \frac{I_{out}^2}{V_{TE2}^2} \frac{N_f}{W_2 L_2} (1 + k_M) \frac{1}{f} \quad (1.20)$$

Equations (1.16) and (1.20) give the thermal and flicker components of the output currents. We will discuss them later. Here, we will focus on another important performance parameter, which is pertinent when the mirror is used to process signals. This parameter is the dynamic range (DR), given by the ratio:

$$DR = \frac{i_{out-FS}}{i_{np-p}} \quad (1.21)$$

where  $i_{out-FS}$  is the full scale excursion of the input current, while  $i_{np-p}$  is the peak-to-peak value of the output noise current. Figure 1.6 shows a possible time diagram of the output current, including the signal (supposed to be sinusoidal) superimposed to a quiescent value  $I_{out-Q}$  (operating point current).

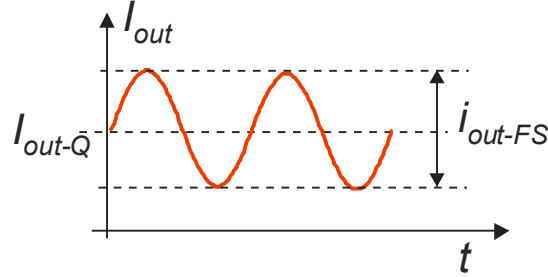


Fig.1.6. Quiescent and signal components of the output current

It can be easily understood that the theoretical maximum full scale current is  $2I_{out-Q}$ . However, to reach this value we should accept that the mirror current gets very close to zero when the signal is at its negative peaks. Generally, this is not possible, since the  $g_m$  of the input devices would also tend to zero and, considering Eq.(1.5), the singularities (pole and zero) would shift to very low frequencies, thus slowing down the mirror response. The consequence would be high distortion and prolonged settling times. For this reason, the full scale current should be represented by:

$$i_{out-FS} = \alpha I_{out-Q} \tag{1.22}$$

with  $\alpha < 2$ . In order to guarantee a wide margin and moderate parameter variations,  $\alpha \leq 1$ . If a value of exactly equal to 1 is used, then the DR coincides with the ratio between the quiescent current and the current noise. This is pertinent when the mirror has only to provide a constant current for biasing purposes. In this particular case, the DR indicates how many times the noise is smaller than the output d.c. current.

The peak-to-peak noise can be approximated to:

$$i_{np-p} = 4i_{n-rms} = 4\sqrt{\int_{f_L}^{f_H} S_{I_{out}}(f)df} \tag{1.23}$$

where  $f_L$  and  $f_H$  are the lower and upper frequency limits of the signal frequency band, respectively. We will consider two different cases, corresponding to the presence of pure flicker or pure thermal noise.

In the case of thermal noise, using (1.16):

$$(DR)^2 = \frac{i_{out-FS}^2}{i_{n-pp}^2} = \frac{\alpha^2 I_{out-Q}^2}{16 \frac{8}{3} kT \frac{I_{out-Q}}{V_{TE2}} (1+k_M) B_S} = \frac{3}{128} \frac{V_{TE2} \alpha^2 I_{out-Q}}{kTB_S (1+k_M)} \tag{1.24}$$

where  $B_S=f_H-f_L$ .

In the case of flicker noise, using Eq.(1.20):

$$(DR)^2 = \frac{\alpha^2 I_{out-Q}^2}{16 \frac{I_{out-Q}^2}{V_{TE2}^2} \frac{N_f}{W_2 L_2} (1+k_M) \ln\left(\frac{f_H}{f_L}\right)} = \frac{\alpha^2 V_{TE2}^2 W_2 L_2}{16 N_f (1+k_M) \ln(f_H / f_L)} \quad (1.25)$$

The results obtained so far are summarized in Table 1.1.

	Output current PSD	DR <sup>2</sup>
Thermal Noise	$\frac{8}{3} kT \frac{I_{out}}{V_{TE2}} (1+k_M)$	$\frac{3}{128} \frac{V_{TE2} \alpha^2 I_{out-Q}}{kTB_S (1+k_M)}$
Flicker noise	$\frac{I_{out}^2}{V_{TE2}^2} \frac{N_f}{W_2 L_2} (1+k_M) \frac{1}{f}$	$\frac{\alpha^2 V_{TE2}^2 W_2 L_2}{16 N_f (1+k_M) \ln(f_H / f_L)}$

Table 1.1

Final considerations:

- The output noise PSD can be written as the product of the noise PSD of the output transistors, multiplied by a factor depending on the mirror gain. High current gains ( $k_M$ ) result in higher noise factors. Currents obtained by magnification of a much smaller current are more prone to noise than currents obtained by mirroring a current of the same value.
- For both thermal and flicker noise, higher currents are accompanied by higher noise levels.
- For both thermal and flicker noise, the higher  $V_{TE}$ , the lower the noise. This means that the best option in terms of noise is biasing currents mirror in strong inversion with large  $V_{GS}-V_T$  values. This recommendation improve also the frequency response but leads to worse voltage ranges.
- As far as DR is concerned, both thermal and flicker noise benefit from large  $V_{TE}$  values. The behavior is different in terms of quiescent current: the DR due to thermal noise can be increased by using large bias currents ( $I_{out-Q}$ ), while, in the case of pure flicker noise, the DR is independent of  $I_{out-Q}$  and the only way to improve DR is using large gate areas (WL) for both  $M_1$  and  $M_2$ .



### 1.3 Noise in cascode current mirrors.

The small signal circuit of a Cascode mirror, with the noise current sources of all MOSFETs, is shown in Fig.1.7. It is necessary to calculate the effect of each noise source on the output current  $i_2$ .

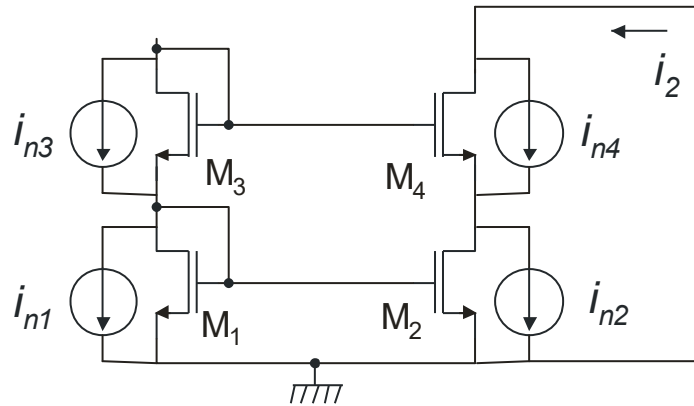


Fig.1.7. Cascode current mirror with noise sources

*Current  $i_{n2}$* : It is split into two components: one flowing into the drain of M2 (resistance  $r_{d2}$ ), the other into the source of M4 (resistance  $1/g_{m4}$ ). Only the latter affects  $i_2$ . The contribution to  $i_2$  is then:

$$i_2(i_{n2}) = i_{n2} \frac{r_{d2}}{r_{d2} + 1/g_{m4}} = \frac{i_{n2}}{1 + \frac{1}{g_{m4}r_{d2}}} \cong i_{n2} \tag{1.26}$$

*Current  $i_{n1}$* : It flows from the source to the drain of M1, and it is mirrored into M2 (multiplied by the current gain  $A_I$  of the mirror, nearly equal to  $=g_{m2}/g_{m1}$ ). This current is transferred from the drain of M2 to the output with a mechanism similar to that of  $i_{n2}$ , the difference being only the sign. Therefore:

$$i_2(i_{n1}) \cong -A_I i_{n1} \tag{1.27}$$

*Current  $i_{n4}$* : This source has not a grounded terminal, so that it should be treated in different way from  $i_{n1}$  and  $i_{n2}$ . To simplify the analysis, we can split this source into two equivalent sources  $i_{n4}'$  and  $i_{n4}''$ , both with a grounded terminal, as shown in Fig. 1.8.

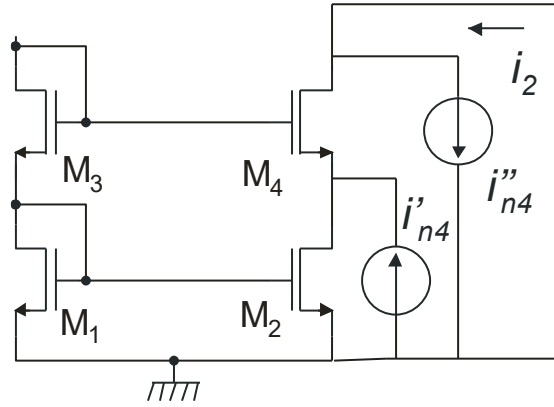


Fig.1.8. Splitting of floating current source  $i_{n4}$  into two components referred to ground

Clearly, the condition to be respected is that  $i_{n4}'$  and  $i_{n4}''$  are equal to  $i_{n4}$ . In this way, we can separately consider the effects of the two sources and then sum up the effects. Source  $i_{n4}''$ , being connected to the output terminal (which is shorted to ground), gives a contribution to  $i_2$  equal to its value, i.e.  $i_{n4}$ . Source  $i_{n4}'$  produces the same effect as  $i_{n2}$ , so that the total effect of  $i_{n4}$  is:

$$i_2(i_{n4}) = i_{n4}'' - i_{n4}' \frac{r_{d2}}{r_{d2} + 1/g_{m4}} = i_{n4} \left( 1 - \frac{r_{d2}}{r_{d2} + 1/g_{m4}} \right) = \frac{i_{n4}}{1 + g_{m4}r_{d2}} \quad (1.28)$$

**Current  $i_{n3}$ .** This current flows only into the diode-connected MOSFET  $M_3$ . The effect is an increase of  $M_3$   $V_{GS}$  equal to  $-i_{n3}/g_{m3}$ . This variation is applied to the gate of  $M_4$ , which operates like a source follower, loaded by  $M_2$ , i.e. by  $r_{d2}$ . The variation on  $M_2$  drain voltage is then:

$$v_{d2} = -\frac{i_{n3}}{g_{m3}} \frac{g_{m4}r_{d2}}{(1 + g_{m4}r_{d2})} \quad (1.29)$$

Thus, the contribution to  $i_2$  is  $v_{d2}/r_{d2}$ , equal to:

$$i_2(i_{n3}) = -i_{n3} \frac{g_{m4}}{g_{m3}} \frac{1}{(1 + g_{m4}r_{d2})} \quad (1.30)$$

Note that cascode Mirrors are generally designed in such a way that  $\beta_2/\beta_1 = \beta_3/\beta_4$ , in order to make the overdrive voltages of  $M_3$  and  $M_4$  equal. In these conditions  $g_{m4}/g_{m3} = g_{m2}/g_{m1} = A_I(0)$

Final considerations.

- The effect of MOSFETS  $M_1$ - $M_2$  is practically equal to that of a simple (non-cascode) current mirror, that is Eq.(1.11) and the following discussion are applicable to also noise currents  $i_{n1}$  and  $i_{n2}$ .

- The noise currents of  $M_3$  and  $M_4$  reach  $i_2$  through a coefficient  $1/(1+g_{m4}r_{d2})$ , therefore, as long as  $g_{m4}r_{d2} \gg 1$ , their effects are strongly attenuated. As a result, their contribution can be neglected in most practical cases.

### 1.4 Wide swing cascode with precise current gain.

Conventional cascode mirrors based on the topology of Fig. 1.7 suffer from two important drawbacks, namely (i) relatively high minimum output voltage ( $V_{min}=V_{GS}+V_{DSAT}$ ) and (ii) quite high input voltage ( $V_{in}=2V_{GS}$ ). The six MOSFET mirror shown in Fig. 1.9 solves the problem of the output voltage range, since  $V_{min}$  can be designed to be as small as  $2V_{DSAT}$ . Unfortunately, its precision is poor, since  $M_2$  and  $M_1$  has different  $V_{DS}$ . Furthermore, the input voltage is still  $2V_{GS}$ .

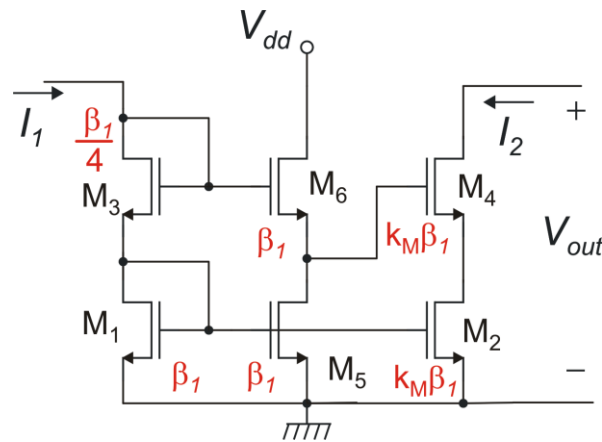


Fig.1.9. Low precision, wide swing cascode current mirror

The cascode mirror shown in Fig.1.10 (a) solves all these problems. It requires an auxiliary voltage,  $V_k$ , to bias the gates of  $M_3$  and  $M_4$ . To study this circuit, we can start by writing  $V_{DS1}$  and  $V_{DS2}$ :

$$\begin{aligned} V_{DS1} &= V_k - V_{GS3} \\ V_{DS2} &= V_k - V_{GS4} \end{aligned} \tag{1.31}$$

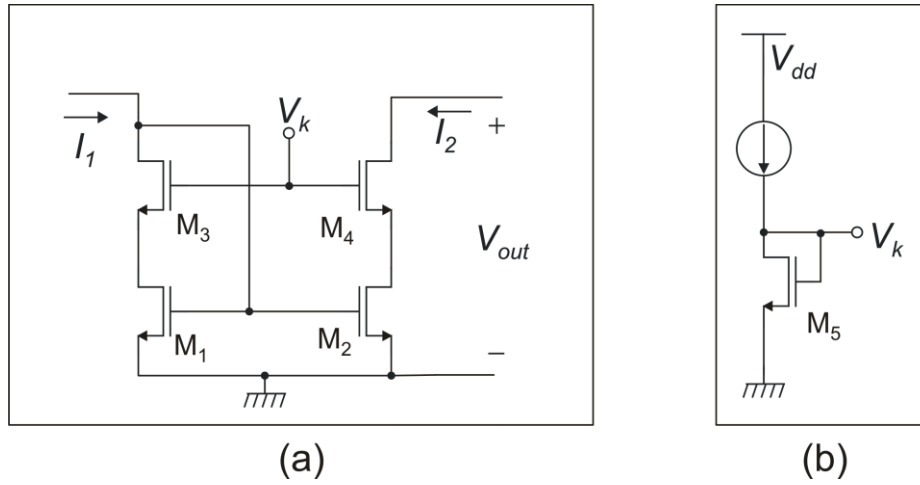


Fig.1.10. (a) High precision, wide swing cascode current mirror with low input voltage. (b) Generation of bias voltage  $V_k$

Choosing  $\beta_4/\beta_3=\beta_2/\beta_1=k_M$ , we obtain  $V_{GS3}=V_{GS4}$ , as in a conventional cascode, so that  $V_{DS1}=V_{DS2}$ . This relationship guarantees that the mirror is precise, in the sense that the actual current gain is equal to the ratio  $\beta_2/\beta_1$ . Voltage  $V_k$  should be chosen to keep  $M_1$  and  $M_2$  in saturation region. Therefore:

$$V_k \geq V_{DSAT2} + V_{GS4} \quad (1.32)$$

Voltage  $V_k$  can be properly chosen to make  $V_{DS1}$  and  $V_{DS2}$  close to the transition to triode region, so that:

$$V_{DS2} \cong V_{DSAT2} = V_{GS2} - V_t \quad \Rightarrow \quad V_{min} \cong V_{DSAT2} + V_{DSAT4} \quad (1.33)$$

In this way,  $V_{min}$  is only equal to  $2V_{DSAT}$ . The condition on  $V_k$  becomes:

$$V_k = V_{DS2} + V_{GS4} = (V_{GS} - V_t)_2 + (V_{GS} - V_t)_4 + V_{t4} \quad (1.34)$$

Voltage  $V_k$  can be produced by the circuit shown in Fig.1.10 (b). Considering Eq.(1.34) we can write:

$$V_k = V_{GS5} = V_{t5} + (V_{GS} - V_t)_5 = (V_{GS} - V_t)_2 + (V_{GS} - V_t)_4 + V_{t4} \quad (1.35)$$

Note that the source of  $M_5$  is grounded, while  $M_4$  source is at potential  $V_{DS2}$ , which, being close to  $V_{DSAT2}$ , is of the order of a few hundred millivolts. Therefore, the body effect on  $V_{t4}$  is small and we can consider that  $V_{t4} \cong V_{t5}$ . Then:

$$(V_{GS} - V_t)_5 = (V_{GS} - V_t)_2 + (V_{GS} - V_t)_4 \quad (1.36)$$

Current  $I_{bias}$  and  $M_5$  aspect ratio ( $W/L$ ) should be properly designed to obtain equality (1.36). Voltage  $V_k$  should also keep  $M_3$  in saturation region. Note that  $V_{D3}=V_{GS1}$ . Therefore, we must guarantee that:

$$V_{D3} = V_{GS1} \geq V_k - V_{t3} = V_k - V_{t4} \quad (1.37)$$

where  $V_{i3}=V_{t4}$  derive from the property  $V_{S3}=V_{S4}$ . Substituting the expression of  $V_k$  from (1.35) we obtain the condition:

$$V_{GS1} \geq (V_{GS} - V_t)_1 + (V_{GS} - V_t)_3 \quad (1.38)$$

which can be further simplified in:

$$V_{t1} \geq (V_{GS} - V_t)_3 \quad (1.39)$$

With the typical value of the threshold voltages in CMOS processes (hundred millivolts), condition (1.39) can be easily satisfied by setting  $(V_{GS}-V_t)_3 = 100$  mV, i.e. by biasing M3 at the boundary between strong and weak inversion.

Finally, we note that the input voltage is simply equal to  $V_{GS1}$ , like in simple current mirrors.

Final considerations.

- The wide-swing cascode current mirror shown in Fig.1.10 offers a low  $V_{min}$  ( $V_{min}=2V_{DSAT}$ ), relatively low input voltage ( $V_{in}=V_{GS}$ ), and also a precise current gain.
- This mirror requires accurate design in order to satisfy (1.33) over the whole range of input currents.